Electrospray Ionization Mass Spectrometry Investigation of Reversible Addition Fragmentation Chain Transfer Mediated Acrylate Polymerizations Initiated via ^{60}Co γ-Irradiation: Mapping Reaction Pathways

Tara M. Lovestead, Gene Hart-Smith, Thomas P. Davis, Martina H. Stenzel,* and Christopher Barner-Kowollik*

Centre for Advanced Macromolecular Design, School of Chemical Sciences and Engineering, The University of New South Wales, Sydney, New South Wales 2052, Australia

Received January 18, 2007; Revised Manuscript Received March 27, 2007

ABSTRACT: Reversible addition fragmentation chain transfer (RAFT) mediated methyl acrylate and butyl acrylate polymerizations initiated via ^{60}Co γ-irradiation were investigated using electrospray ionization mass spectrometry (ESI−MS). The polymer end-groupings were mapped using both a hybrid quadrupole-time-of-flight instrument and a quadrupole ion trap mass spectrometer. Three potential initiation processes were identified during the cumyl phenyl dithioacetate (CPDA) mediated acrylate polymerizations. CPDA dissociates into a cumyl radical and a phenyl dithioester radical (Z-group). A set of polymer product ions indicates that a small, yet significant, fraction of the γ-generated phenyl dithioacetate radical contributes to the initiation process. Furthermore, the phenyl dithioacetate group undergoes cleavage to yield thiol end groups that react to form disulfide linkages. Additionally, polymer product ions indicative of a small amount of water radiolysis were observed, and evidence that the butyl acrylate monomer interacts with γ-radiation to yield an initiating species is gained.

Introduction

Free radical polymerization (FRP) initiated via ^{60}Co γ-irradiation is attractive for grafting monomer onto polymer backbones, polymerization of composites, cross-linking polymer chains, and synthesizing copolymers as well as modifying polymer properties because a constant ionizing energy source supplies a constant radical species concentration.[1−8] Additionally, γ-radiation affords an environmentally friendly alternative to thermally initiated polymerizations as this process occurs at ambient temperatures. Reversible addition fragmentation chain transfer (RAFT) chemistry is used routinely to generate functional and complex molecular architectures, such as block copolymers, core−shell nanoparticles, branched structures, as well as star and graft polymers.[9−12] Recently, RAFT chemistry has been used in conjunction with γ-initiation for the synthesis of complex polymer systems for the generation of extremely well-defined polymers with respect to polydispersity and molecular weight as well as for the construction of polymer−protein conjugates;[13−19] however, the exact initiation pathway is unclear.

FRPs in the presence of RAFT agents is generally accepted to occur via the reaction mechanisms presented in Scheme 1, although direct evidence for cross-termination (reactions Vc and Vd in Scheme 1) has not been established.[20] Reaction I entails the generation of an initiating species, I•, (Ia), from a small molecular weight species, which, in this case, must arise from γ-interactions with the monomer and RAFT agent under ambient conditions. Upon monomer, M, addition, I• forms a primary radical, P_1•, (Ib), which proceeds with an initiation rate coefficient, k_i. Reactions II and IV are unique to RAFT polymerizations and represent the pre-equilibrium (where the initial RAFT agent reacts with a polymeric chain of arbitrary chain length *i* or *j* (i.e., P_i or P_j) to form the macroRAFT agent) and the core equilibrium (where the polyRAFT species grows uniformly with monomer to polymer conversion). The pre-equilibrium also entails monomer addition to the RAFT agent-derived radicals, R•, which proceeds with a rate coefficient, $k_{p,rein}$. The pre-equilibrium and the core equilibrium are governed by

Scheme 1. Reactions[a] Describing the Reversible Addition Fragmentation Chain Transfer (RAFT) Process Initiated via ^{60}Co γ-Irradiation[11,21]

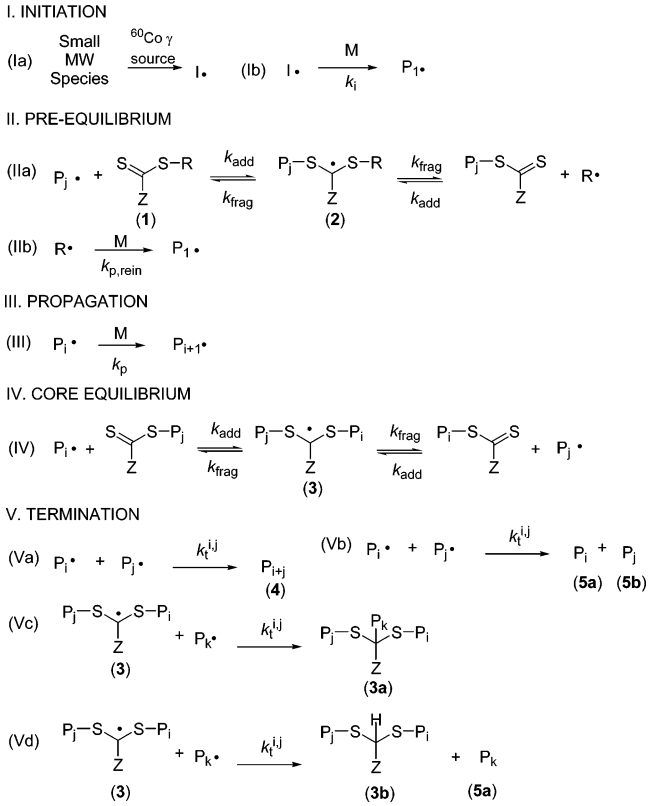

[a] Note that the initiating species is unknown and cross-termination (reactions **Vc** and **Vd**) has not been observed during CPDA mediated RAFT polymerization.[22−25]

* Corresponding authors. E-mail: (Centre for Advanced Macromolecular Design) camd@unsw.edu.au; (M.H.S.) m.stenzel@unsw.edu.au; (C.B.-K.) c.barner-kowollik@unsw.edu.au. Fax: 61.2.9385.6250. Telephone: 61.2.9385.4331.

10.1021/ma0701484 CCC: $37.00
Published on Web 05/18/2007

Scheme 2. Basic Reactions Describing the Reversible Termination Process

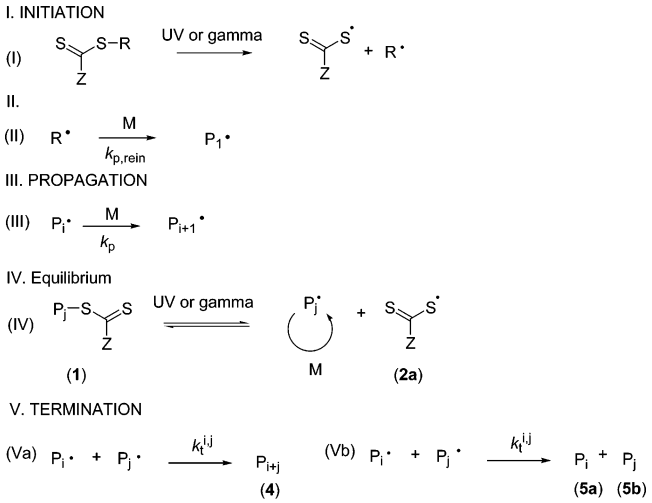

the magnitude of the addition and fragmentation rate coefficients (k_{add} and k_{frag}). Several small molecular weight species may form initiating species that can enter the pre-equilibrium reaction II. Reactions III and V represent the conventional FRP propagation and termination reactions, respectively. Here (Va) and (Vc) represent termination by combination and (Vb) and (Vd) represent termination by disproportionation, which are governed by a chain length dependent termination rate coefficient, i.e., $k_t^{i,j}$, albeit, once again, direct evidence for the cross-termination reactions Vc and Vd has not been established.[20]

While the RAFT mechanism is generally accepted to explain the controlled/"living" FRP behavior observed during ^{60}Co γ-irradiation in the presence of thiocarbonylthio compounds, reversible termination (Scheme 2) has also been proposed as the mechanism that imparts controlled growth.[26] Reversible termination proceeds via dissociation of the dithiocarbonate compound into a stable dithioester radical and R• (Scheme 2, reaction I), the initiating species that generates the primary radicals (reaction II), which propagate and terminate according to conventional FRP kinetics (reactions III and V, respectively). Reaction IV details the controlling mechanism, i.e., a reversible activation/deactivation sequence between the polymer chain end-capped by the dithioester group (**1**) and the growing polymer chain and the stable dithioester radical species (**2a**).

In spite of numerous applications for controlled/"living" FRPs initiated via γ-irradiation, the initiating species and/or initiation mechanism remain unclear. Mass spectrometric techniques such as matrix assisted laser desorption ionization−time-of-flight−mass spectrometry (MALDI−ToF−MS) and electrospray ionization−MS (ESI−MS) are often employed to analyze and characterize synthetic polymers.[27−37] While MALDI−ToF−MS can be used to examine a significantly larger mass to charge ratio (m/z) compared to ESI−MS (i.e., m/z up to ∼100 000 compared to ∼2000 Da, respectively, for singly charged species), ESI−MS is a soft ionization method, and thus, virtually no fragmentation of the polymer chain and/or chain end-grouping occurs. In contrast, MALDI−ToF−MS (also a soft ionization technique) has been shown to cause the polymer end-groupings of RAFT mediated polymer chains to fragment.[34] Additionally, isotopic pattern resolution and m/z value accuracy of up to 0.01 Da is achieved using certain ESI−MS techniques.

Previously, ESI−MS has been used to study the mechanistic aspects of (living) FRPs[21,31,38−41] as well as to conduct fundamental kinetic investigations of conventional polymerization.[42−44] The RAFT agent cumyl phenyl dithioacetate (CPDA) was selected because it imparts minimal rate retardation effects.[21,45] Additionally, methyl acrylate (MA) and butyl acrylate (BA) undergo controlled/"living" polymerization during ^{60}Co γ-irradiation,[26,46−50] ionize well under ESI conditions and are low in repeat unit molecular weight (i.e., can yield polymer product within the ESI−MS detection limits).[21,41] The present contribution aims at addressing the significant gap in mechanistic knowledge by directly mapping the polymeric product spectrum obtained in γ-radiation induced free radical polymerization under RAFT control. The study provides detailed mechanistic insights into the initiating species while concomitantly advancing the boundaries of polymer analysis via electrospray ionization mass spectrometry.

Experimental Section

Materials. Methyl acrylate (Aldrich, 99%) and butyl acrylate (Aldrich, 99%) were purified by passing through a column of basic alumina and distillation prior to use. Cumyl phenyl dithioacetate was synthesized and characterized using the CAMD method of Quinn et al.[25,51] Toluene was used after drying over a molecular sieve (3A).

Polymerization. Bulk BA and MA and the 50/50 vol % BA/toluene samples were prepared with 0.02 M CPDA in glass vials, sealed with rubber septa and copper wire and deoxygenated via N_2 purging for 20 min. Samples were placed in a sealed room with a ^{60}Co source that operates at room temperature on a revolving platform to ensure uniform irradiation at a dose rate of 0.11 kGy h^{-1}.[52] Samples were removed from the γ-source at predetermined time points that were selected to obtain low molecular weight polymer. For example, to achieve polymer product of approximately 3% conversion, 9 h, 13 h, or 7 days of γ-radiation was required for the bulk MA, bulk BA, and the 50/50 vol % BA/toluene samples, respectively. Upon removal, conversion was determined gravimetrically after drying in a fume hood.

Mass Analysis. Obtaining mechanistic information from ESI−MS first requires identification of the polymer product ions. The minor peaks, i.e., those that exist in small quantities compared with the main polymer product ion (species **1**, Scheme 3), afford the most valuable mechanistic information because they are termination products, which provide indirect information about the initiation processes. Thus, to aid in identifying the important (minor) peaks, two soft-ionization mass spectrometric techniques were used. First, an Ultima hybrid quadrupole-time-of-flight (Q-ToF) instrument (Micromass, Altrincham, Cheshire, UK) equipped with a ZSpray sample introduction system in a nanoflow electrospray ion source was used in positive ion mode with a source temperature of 200 °C. Mass calibration was performed using the fragment ions of Glu-fibrino peptide. Samples were delivered into the ion source from nanospray emitters (Proxeon, Odense, Denmark). The cone voltage off-set was set at 50 V and the system was operated with a capillary voltage of around 800 V. All spectra were acquired via the ToF analyzer and were integrated every 2.4 s over the mass-to-charge, m/z, range 50−2000 Da. Data were recorded and processed using the MassLynx software, version 4.0.

Additionally, a Thermo Finnigan LCQ Deca quadrupole ion trap mass spectrometer (Thermo Finnigan, San Jose, CA) equipped with an atmospheric pressure ionization source operating in the nebulizer assisted electrospray mode was used in positive ion mode. Mass calibration was performed using caffeine, MRFA (Sigma-Aldrich) and Ultramark 1621 (Sigma-Aldrich) in the m/z range 195−1822 Da. All spectra were acquired over the m/z range 150−2000 Da with a spray voltage of 5 kV, a capillary voltage of 26 V, and a capillary temperature of 275 °C. Nitrogen was used as sheath gas (flow: 50% of maximum) and helium was used as auxiliary gas (flow: 5% of maximum).

The eluent was a 6:4 v/v mixture of THF:methanol with an acetic acid concentration of 0.1 mM. Acetic acid was added to the solvent prior to analysis to ensure that ionization would occur, albeit ionization occurs readily from the sodium content that occurs

Scheme 3. Select Sodium Adducts of the Expected Polymer Product Ions from Electrospray if the Cumyl Phenyl Dithioacetate Mediated Methyl Acrylate Polymerization Proceeds According to the Reaction Mechanisms Presented in Scheme 1

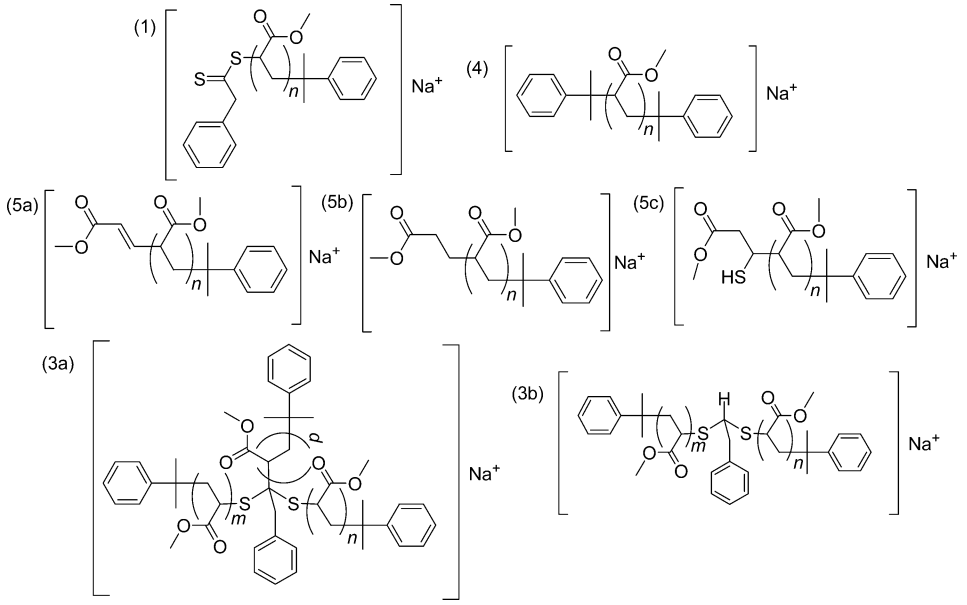

naturally in the glass. The peak masses do shift upon potassium salt addition; however, the overall signal strength decreases do to blockage of the heated capillary. Thus, since sodiated peaks occur when neat solvents are used, no metal salts were added. Additionally, each spectrum was examined for the presence of the main polymer product ion for several potential metal cations, salt clusters and/or solvent molecule attachments.[32] All theoretical molecular weights were calculated using the exact mass as provided by the program package CS ChemDraw 6.0 for the first peak in any given isotopic pattern. The theoretical isotopic patterns were generated using the Xcalibur program included with the Thermo Finnigan LCQ Deca ion trap mass spectrometer.

Results and Discussion

Methyl Acrylate:Quadrupole Ion Trap Mass Spectrometer. Initially, a quadrupole ion trap mass spectrometer was used to investigate the polymer product spectrum of the RAFT-mediated bulk methyl acrylate polymerization initiated via ^{60}Co γ-irradiation (Figure 1, upper part). Also presented in Figure 1

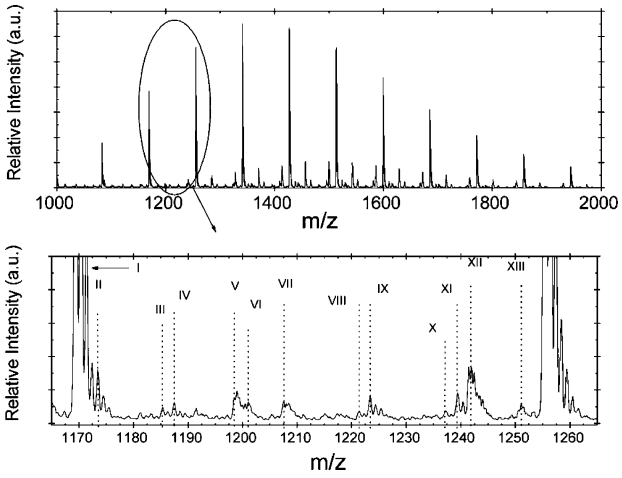

Figure 1. Spectrum of poly(methyl acrylate) obtained from electrospray ionization mass spectrometry of a reversible addition fragmentation chain transfer mediated MA polymerization initiated via ^{60}Co γ-irradiation at room temperature. The lower graph presents an expanded view of the mass range 1165−1265 Da, where the *y*-axis is scaled to allow for better viewing of the minor peaks. Polymer products were analyzed using a quadrupole ion trap mass spectrometer.

Table 1. Polymer Peaks for the Spectrum of Poly(methyl acrylate) Obtained from the Reversible Addition Fragmentation Chain Transfer Mediated MA Polymerization Initiated via ^{60}Co γ-Irradiation at Room Temperature and Analyzed Using a Quadrupole Ion Trap Mass Spectrometer (Figure 1) along with Normalized Peak Intensities (norm. int., Normalized to the Peak Intensity of Species 1, Scheme 3), the Experimental and Theoretical *m*/*z* Values (m/z_{exp} and m/z_{theo}, Respectively), the Ion Assignments (ion assign.), the Molecular Formulas, the Number of Monomer Units Associated with the Ion Assignments (*n*), and the *m*/*z* Errors[a]

peak	norm. int.	m/z_{exp}	ion assign.	molecular formula	*n*	m/z_{theo}	$m/z_{exp} - m/z_{theo}$
I	1.00	1169.41	**1**	$[C_{57}H_{78}O_{20}S_2 + Na]^+$	10	1169.442	−0.04
II	0.09	1173.49	**5a**	$[C_{57}H_{82}O_{24} + Na]^+$	12	1173.509	−0.02
			18a	$[C_{52}H_{78}O_{28} + Na]^+$	13	1173.457	0.03
			12g	$[C_{52}H_{78}O_{26}S + Na]^+$	13	1173.439	0.05
III	0.02	1185.33	**1b**	$[C_{57}H_{78}O_{21}S_2 + Na]^+$	10	1185.437	−0.10
IV	0.03	1187.45					
V	0.04	1198.47	**1**	$[C_{113}H_{162}O_{48}S_2 + Na_2]^{2+}$	24	1198.473	−0.01
VI	0.03	1201.05					
VII	0.03	1207.53	**1d**	$[C_{57}H_{84}O_{24}S + Na]^+$	12	1207.497	0.03
			4	$[C_{62}H_{88}O_{22} + Na]^+$	11	1207.566	−0.04
			7e	$[C_{56}H_{80}O_{25}S + Na]^+$	12	1207.460	0.07
			18	$[C_{52}H_{80}O_{30} + Na]^+$	13	1207.460	0.07
VIII	0.02	1221.39	**7a**	$[C_{56}H_{78}O_{24}S_2 + Na]^+$	12	1221.422	−0.03
IX	0.04	1223.39	**7b**	$[C_{56}H_{80}O_{24}S_2 + Na]^+$	12	1223.437	-0.05
X	0.02	1237.29					
XI	0.05	1239.44	**1a**	$[C_{61}H_{84}O_{23}S + Na]^+$	11	1239.502	−0.06
			12b	$[C_{57}H_{84}O_{24}S_2 + Na]^+$	12	1239.469	−0.03
			7h	$[C_{56}H_{80}O_{25}S_2 + Na]^+$	12	1239.432	0.01
XII	0.09	1241.47	**1**	$[C_{117}H_{168}O_{50}S_2 + Na_2]^{2+}$	25	1241.491	−0.02
XIII	0.03	1251.07					

[a] See Schemes 3−6 for the corresponding product ion structures.

is an expanded view of the mass range 1165−1275 Da, which was selected because it adequately represents the polymer product (lower part, where the *y*-axis is scaled to allow for better viewing of the minor peaks). The peaks that appear in a typical pattern are labeled with a Roman numeral. Additionally, Table 1 displays the polymer peaks indicated in Figure 1 along with their normalized peak intensities (normalized to the polymer product ion intensity of species **1**, Scheme 3), the experimental and theoretical *m*/*z* values (m/z_{exp} and m/z_{theo}, respectively), the polymer ion assignments, the corresponding molecular formulas, the number of monomer units associated with the ion assignments (*n*) and the *m*/*z* errors.

Figure 1 clearly shows two polymer distributions (upper part). The main polymer distribution is product ion **1**, the cumyl

Scheme 4. Sodium Adducts from Electrospray of Cumyl Phenyl Dithioacetate Mediated Methyl Acrylate Polymer Initiated via ^{60}Co γ-Irradiation: Variants of Species 1

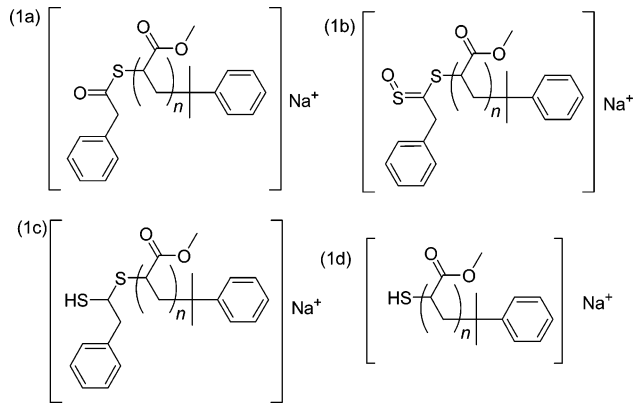

initiated polymer chain end-capped with phenyl dithioacetate (peak I). The second distribution arises from double charging of this main polymer product ion **1** due to attachment of two sodium ions and includes product ion peaks V and XII (see Scheme 3, which presents select sodium adducts expected from electrospray if the CPDA-mediated methyl acrylate polymerization proceeds according to the reaction mechanisms presented in Scheme 1). Additionally, peak III is the polymer product ion (**1b**) (Scheme 4). This ion has also been observed for thermally initiated RAFT-mediated acrylate polymerizations[41] and arises from oxidation due to peroxides present in the THF (used for ESI−MS sample preparation). Scheme 4 presents potential analogues of the main RAFT-mediated MA polymer product species **1** that arise from either oxidation due to peroxides in the THF (**1a** and **1b**), reduction of the C═S bond (**1c**) or cleavage of the carbon sulfur linkage in the Z-group (**1d**). Throughout this paper, polymer product ions that are found within instrumental error are presented; however, for a more complete list of all potential product ions and their corresponding analogues, the interested reader is referred to the Supporting Information section.

Table 1 shows that multiple ion assignments exist for peaks II, VII, and XI because the molar masses for the different ion structures differ by less than the instrument error (∼0.1 Da for the LCQ Deca ion trap). For example, peak VII can be either the polymer product ion **1d**, which may result from the RAFT agent interacting with the γ-radiation; species **4**, the cumyl initiated polymer terminated via combination; species **7e**, an analogue of the set of product ions that result from dithioester initiated polymer terminated via disproportionation, **7a** and **7b** (see Schemes 4, 3, and 5, respectively); or species **18**, which may form if peroxy initiation is important. Species **7b** may form also via chain transfer to monomer and subsequent reaction with the RAFT agent; however, this mechanism does not account for formation of species **7a**. A more complete list of potential dithioester initiated polymer product ion analogues that terminate via either disproportionation (Scheme S1) or combination (Scheme S2) are presented in the Supporting Information section.

In addition to species **7e**, polymer product ions **7a** and **7b** are observed (Figure 1 peaks VIII and IX, respectively) suggesting that a small percentage of the dithioester radicals may initiate polymer chains. This hypothesis is corroborated further by peak XI, which is either species **1a**, **7h**, or **12b** (see Schemes 4, 5, and 6, respectively). The possibility of polymer product ion **12b** indicates that both polymer product ions **1d** and **12h** (Scheme 6) are formed but that their thiol end groups

Scheme 5. Sodium Adducts from Electrospray of Cumyl Phenyl Dithioacetate Mediated Methyl Acrylate Polymer Initiated via ^{60}Co γ-Irradiation: Dithioester Initiated Polymer Terminated via Disproportionation[a]

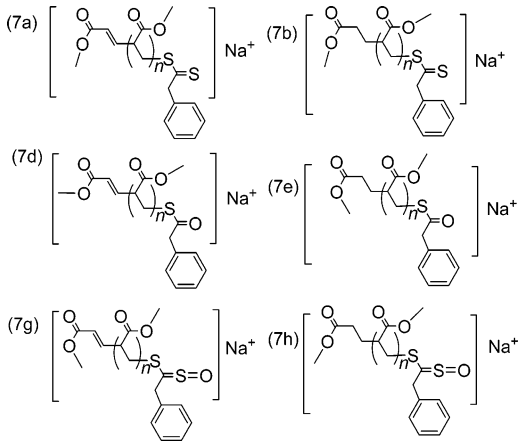

[a] Please see Schemes S1 and S2 in the Supporting Information for a more complete list of potential dithioester initiated polymer product ion analogues that terminate via either disproportionation (Scheme S1) or combination (Scheme S2)

react to form a disulfide bond. For a more complete list of potential polymer product ions involving thiol end group and/or disulfide bond formation please see Scheme S3 in the Supporting Information section.

Multiple polymer ion assignments also exist for peak II, which may be either a cumyl initiated disproportionation product ion (**5a**) (Scheme 3), a peroxy initiated disproportionation polymer product ion (**18a**) (Scheme 6) or a thiol initiated disproportionation polymer product ion (**12g**) (Scheme 6). Peaks IV, VI, X, and XIII remain unknown.

Methyl Acrylate:Hybrid Quadrupole−Time-of-Flight Mass Spectrometer. To investigate further the RAFT-mediated MA polymerizations initiated via ^{60}Co γ-irradiation, specifically, the unknown peaks (IV, VI, X, and XIII), the peaks with multiple ion assignments (peaks II, VII, VIII, and XI) and the importance of dithioester initiation, a Q−ToF instrument was used to examine the polymer product. This instrument operates in nanospray mode and uses ToF principles, and thus, is able to resolve product peaks with excellent isotopic pattern resolution. Additionally, an internal calibration can be utilized to improve m/z accuracy. Thus, since the molecular weights for the main polymer product ion (**1**) at various degrees of polymerization are known, the instrument was calibrated using these values and a m/z accuracy of ∼0.01 Da for peaks of similar intensity and ∼0.05 Da for peaks of much less or much greater intensity is possible. Since the interesting peaks, at least from a mechanistic viewpoint, are typically much less intense than the main polymer product peaks, a second calibration was made using the second isotope for species **1**, which is much weaker in signal intensity. Thus, m/z accuracy for all peaks regardless of intensity of ∼0.01 Da is possible.

Figure 2 presents the polymer product spectra obtained using a Q−ToF instrument for the same CPDA-mediated MA polymerization initiated via ^{60}Co γ-irradiation as presented in Figure 1. The theoretical isotopic pattern for the polymer product ions (upper part) is also presented. Table 2 shows the normalized peak intensities (normalized to the main peak); both m/z_{exp} values obtained when the sample is calibrated using either the main peak or the second isotope (m/z_{exp1} or m/z_{exp2},respectively), the polymeric product ion assignments, the corresponding molecular formulas, the theoretical m/z values and the respective

Scheme 6. Sodium Adducts from Electrospray of Cumyl Phenyl Dithioacetate Mediated Methyl Acrylate Polymer Initiated via ^{60}Co γ-Irradiation: Thiol End group and/or Disulfide Bond Formation[a]

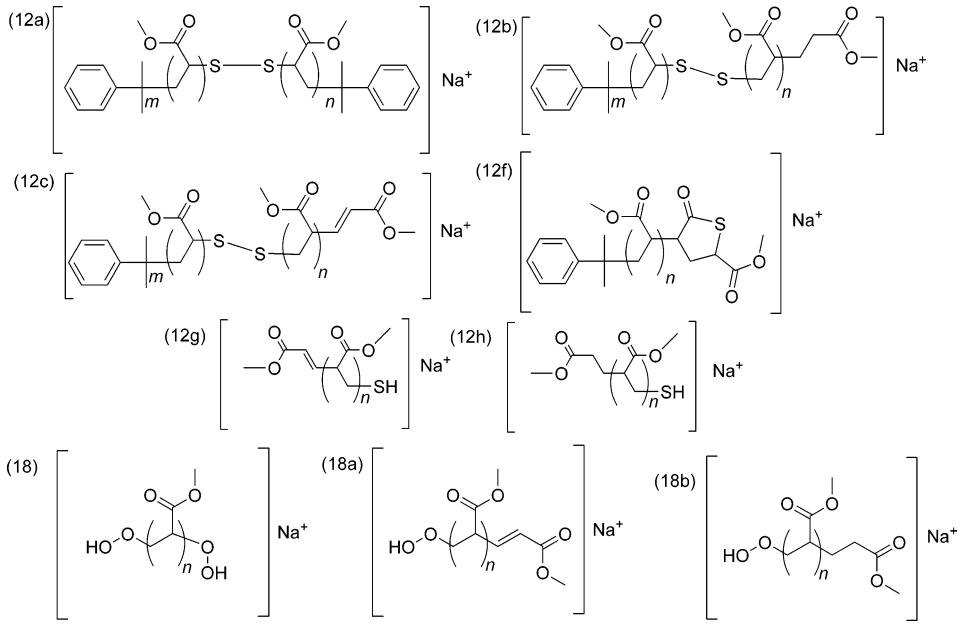

[a] Please see Scheme S3 in the Supporting Information for a more complete list.

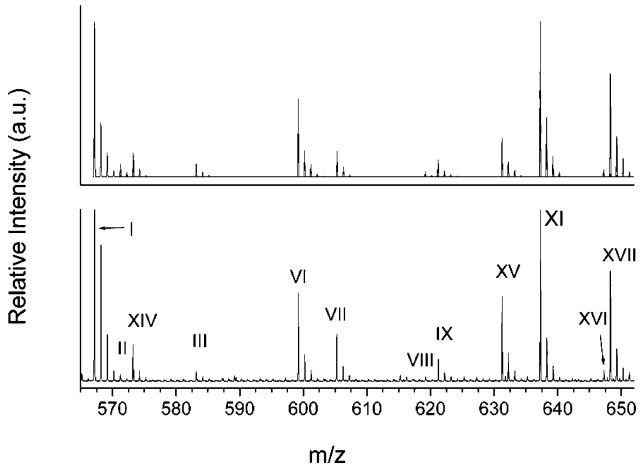

Figure 2. Spectrum of poly(methyl acrylate) obtained from the electrospray ionization mass spectrometry of a reversible addition fragmentation chain transfer mediated MA polymerization initiated via ^{60}Co γ-irradiation at room temperature. The lower graph presents an expanded view in the mass range 565−655 Da, characteristic of the polymer product spectrum. The upper part presents the theoretical isotopic pattern for the polymer product ions. Polymer products were analyzed using a hybrid quadrupole-time-of-flight mass spectrometer.

errors for either calibration. While the mass range presented in Figure 2 is different from that of Figure 1, the mass range that represents the highest degree of polymerization and lowest extent of double charging (which significantly complicates the spectrum) is displayed, and all peaks that repeat throughout the spectrum are presented to ensure an adequate representation of the polymer product ions.

Excellent resolution of the individual peaks to baseline with clear isotopic patterns was obtained with a Q−ToF instrument (Figure 2). Additionally, identical m/z values (±0.01) are obtained regardless of the calibration method used (i.e., whether or not the calibration was made using the main peak or the second isotope of the main peak) except for peak XV. The enhanced signal-to-noise ratio and clear isotopic pattern resolution allows for more exact peak assignments. Upon inspection, Figure 2 and Table 2 corroborate that peaks I, XI, and III, respectively, are the main polymer product ion (**1**) and the oxidized analogues of **1**, **1a**, and **1b**, respectively. Additionally, peak VII is determined unambiguously to be **1d** and the new peaks XV, XVII, and XVI are species **1** cationized by H^+ and NH_4^+, respectively, and species **1b** cationized by H^+.

Most importantly, the dithioester initiated polymer ions (peaks VIII and IX) are again observed. Thus, dithioester radical initiation does occur during CPDA-mediated MA polymerization initiated via ^{60}Co γ-irradiation. This finding suggests that a portion of the RAFT agent cleaves to form Z-groups that initiate polymer chains.

The analysis obtained using the Q−ToF instrument confirms that peak II originates from a cumyl initiated polymer (i.e., product ion **5a**). Additionally, a new peak XIV is observed that is either **5b** (see Scheme 3) or species **13b**, an HO$^\bullet$ initiated polymer (see Scheme 7); however, additional polymer product ions indicative of water radiolysis are not observed, and **5a** and **5b** are disproportionation products that are expected to appear as a set.

The enhanced spectral resolution obtained using the Q−ToF also enables peak VI identification. Two assignments are possible: species **9**, which forms from midchain radical termination along the backbone of the main RAFT product ion **1**,[53] or species **7b** cationized by hydrogen. While the error for assigning this peak to species **9** is less, this peak also appears at even lower molecular weights (i.e., $m/z_{exp} = 427.12$) and thus cannot be assigned to a product ion that requires a higher degree of polymerization to form. Additionally, peak IV is not observed using the Q−ToF instrument. For a more complete list of potential polymer product ions involving long chain branching, please see Schemes S4−S7 in the Supporting Information section.

Butyl Acrylate:Quadrupole Ion Trap Mass Spectrometer. To elucidate further the initiation mechanisms that occur during RAFT-mediated FRPs initiated via ^{60}Co γ-irradiation and, more specifically, the importance of dithioester initiation, this same study was performed using butyl acrylate. While the Q−ToF clearly provides better isotopic pattern resolution when compared to the ion trap instrument, both instruments were used

Table 2. Polymer Peaks along with Normalized Peak Intensities (norm. int., Normalized to the Peak Intensity of Species 1, Scheme 1); m/z_{exp} Values Obtained When the Sample Is Calibrated Using Either the Main Peak or the Second Isotope (m/z_{exp1} or m/z_{exp2}, Respectively); m/z_{theo}; the Ion Assignments (ion assign.); the Molecular Formulas, the Number of Monomer Units Associated with the Ion Assignments (n) and the Respective Errors for Either Calibration Method for the Spectrum of Poly(MA) Obtained from the Reversible Addition Fragmentation Chain Transfer Mediated MA Polymerization Initiated via ^{60}Co γ-Irradiation at Room Temperature and Analyzed Using a Hybrid Quadrupole−Time-of-Flight Mass Spectrometer[a]

peak	norm.int.	$m/z_{exp,1}$	$m/z_{exp,2}$	ion assign.	molecular formula	n	m/z_{theo}	$m/z_{exp,1} - m/z_{theo}$	$m/z_{exp,2} - m/z_{theo}$
I	1.00	567.18	567.18	**1**	$[C_{29}H_{36}O_6S_2 + Na]^+$	3	567.185	0.00	0.00
II	0.01	571.25	571.23	**5a**	$[C_{29}H_{40}O_{10} + Na]^+$	5	571.252	−0.01	−0.02
XIV	0.04	573.24	573.24	**5b**	$[C_{29}H_{42}O_{10} + Na]^+$	5	573.226	0.01	0.01
				13b	$[C_{24}H_{38}O_{14} + Na]^+$	6	573.215	0.02	0.02
III	0.01	583.19	583.19	**1b**	$[C_{29}H_{36}O_7S_2 + Na]^+$	3	583.179	0.02	0.01
VI	0.09	599.22	599.22	**7b**	$[C_{28}H_{38}O_{10}S_2 + H]^+$	5	599.198	0.02	0.02
				9	$[C_{34}H_{40}O_4S_2 + Na]^+$	2	599.227	−0.01	−0.01
VII	0.05	605.25	605.25	**1d**	$[C_{29}H_{42}O_{10}S + Na]^+$	5	605.239	0.01	0.01
VIII	0.01	619.22	619.21	**7a**	$[C_{28}H_{36}O_{10}S_2 + Na]^+$	5	619.165	0.06	0.05
IX	0.03	621.21	621.21	**7b**	$[C_{28}H_{38}O_{10}S_2 + Na]^+$	5	621.180	0.03	0.03
XV	0.08	631.32	631.25	**1**	$[C_{29}H_{36}O_6S_2 + H]^+$	4	631.240	0.08	0.01
XI	0.21	637.27	637.27	**1a**	$[C_{33}H_{42}O_9S + Na]^+$	4	637.244	0.03	0.03
XVI	0.01	647.26	647.27	**1b**	$[C_{33}H_{42}O_9S_2 + H]^+$	4	647.234	0.03	0.03
XVII	0.09	648.28	648.27	**1**	$[C_{29}H_{36}O_6S_2 + NH_4]^+$	4	648.266	0.01	0.00

[a] See Schemes 3−5 and 7 for the corresponding product ion structures.

Scheme 7. Sodium Adducts from Electrospray of Cumyl Phenyl Dithioacetate Mediated Methyl Acrylate Polymer Initiated via ^{60}Co γ-Irradiation: Water Radiolysis and Long Chain Branching[a]

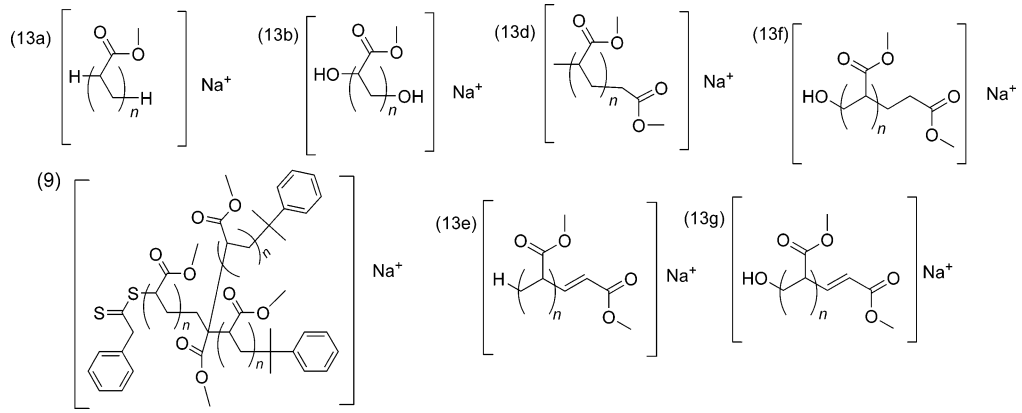

[a] See Schemes S4−S7 in the Supporting Information for a more complete list.

to investigate the poly(BA) mechanism because different polymer product ions appear more clearly using the different mass spectrometers.

Figure 3 presents the polymer product spectrum obtained using the LCQ deca ion trap mass spectrometer for the CPDA-mediated BA polymerization initiated via ^{60}Co γ-irradiation, along with the theoretical isotopic pattern for the polymer product ions (upper part). For ease of data reporting, peak labeling with the roman numerals begins anew with I (lower part, where the y-axis is scaled to allow for better viewing of the minor peaks). Additionally, Table 3 displays the polymer peaks along with the normalized peak intensities (normalized to the peak intensity of species **1**, Scheme 1), the experimental

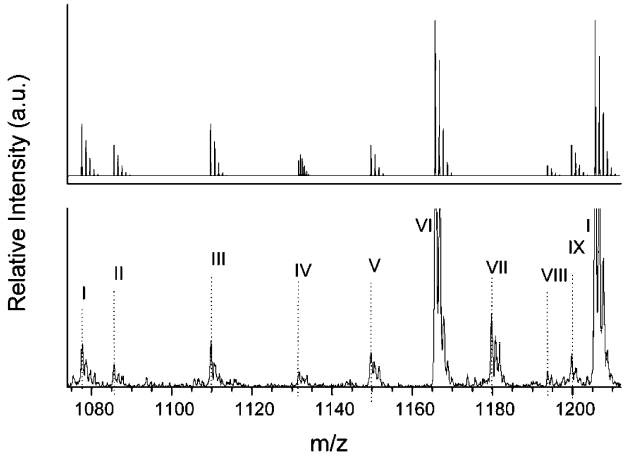

Figure 3. Spectrum of poly(butyl acrylate) obtained from the electrospray ionization mass spectrometry of a reversible addition fragmentation chain transfer mediated BA polymerization initiated via ^{60}Co γ-irradiation at room temperature. The lower graph presents an expanded view of the mass range 1075−1210 Da, characteristic of the entire polymer product spectrum. The upper part presents the theoretical isotopic pattern for the polymer product ions. Polymer products were analyzed using a quadrupole ion trap mass spectrometer.

Table 3. Polymer Peaks along with Normalized Peak Intensities (norm. int., Normalized to the Peak Intensity of Species 1, Scheme 1), the Experimental and Theoretical m/z Values (m/z_{exp} and m/z_{theo}, Respectively), the Ion Assignments (ion assign.), the Molecular Formulas, the Number of Monomer Units Associated with the Ion Assignments (n) and the m/z Errors for Poly(butyl Acrylate) Obtained from the Reversible Addition Fragmentation Chain Transfer Mediated BA Polymerization Initiated via ^{60}Co γ-Irradiation at Room Temperature and Analyzed Using a Quadrupole Ion Trap Mass Spectrometer[a]

peak	norm. int.	m/z_{exp}	ion assign.	molecular formula	n	m/z_{theo}	$m/z_{exp} - m/z_{theo}$
I	0.15	1077.59	**1**	$[C_{59}H_{90}O_{12}S_2 + Na]^+$	6	1077.577	0.01
II	0.09	1085.61	**7a**	$[C_{57}H_{90}O_{14}S_2 + Na]^+$	7	1085.566	0.04
III	0.16	1109.78	**15**	$[C_{58}H_{102}O_{18} + Na]^+$	8	1109.696	0.09
IV	0.06	1131.59	**7b**	$[C_{120}H_{200}O_{32}S_2 + Na_2]^{++}$	16	1131.662	−0.07
V	0.12	1149.73	**17a**	$[C_{61}H_{106}O_{18} + Na]^+$	8	1149.727	0.00
VI	1.00	1165.85	**5a**	$[C_{65}H_{106}O_{16} + Na]^+$	8	1165.737	0.10
VII	0.24	1179.78					
VIII	0.06	1193.74	**13f**	$[C_{63}H_{110}O_{19} + Na]^+$	9	1193.753	−0.01
IX	0.10	1199.78	**1d, 5c**	$[C_{65}H_{108}O_{16}S + Na]^+$	8	1199.725	0.05
I	1.00	1205.68	**1**	$[C_{66}H_{102}O_{14}S_2 + Na]^+$	7	1205.661	0.02

[a] See Schemes 3−5, 7, and 8 for the corresponding structures.

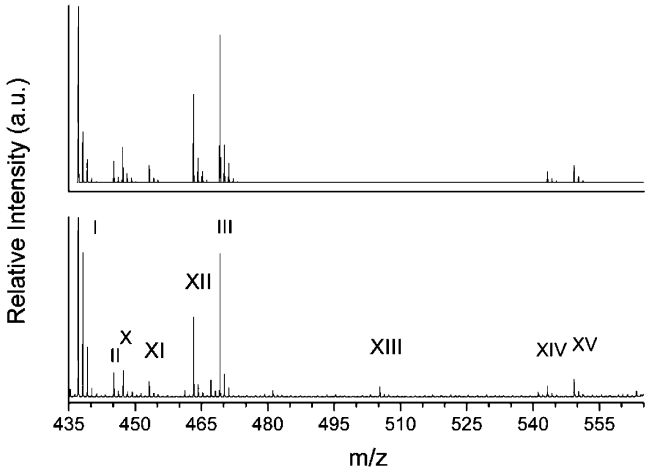

Figure 4. Spectrum of poly(butyl acrylate) obtained from the electrospray ionization mass spectrometry of a reversible addition fragmentation chain transfer mediated BA polymerization initiated via ^{60}Co γ-irradiation at room temperature. The lower part presents an expanded view of the mass range 435−565 Da. The upper part presents the theoretical isotopic pattern for the polymer product ions. Polymer products were analyzed using a hybrid quadrupole-time-of-flight mass spectrometer.

Table 4. Polymer Peaks along with Normalized Peak Intensities (norm. int., Normalized to the Peak Intensity of Species 1, Scheme 1), the Experimental and Theoretical *m*/*z* Values (m/z_{exp} and m/z_{theo}, Respectively), the Ion Assignments (ion assign.), the Molecular Formulas, the Number of Monomer Units Associated with the Ion Assignments (*n*) and the *m*/*z* Errors for Poly(butyl Acrylate) Obtained from the Reversible Addition Fragmentation Chain Transfer Mediated BA Polymerization Initiated via ^{60}Co γ-Irradiation at Room Temperature and Analyzed Using a Hybrid Quadrupole−Time-of-Flight Instrument[a]

peak	norm. int.	m/z_{exp}	ion assign.	molecular formula	*n*	m/z_{theo}	$m/z_{exp} - m/z_{theo}$
I	1.00	437.14	**1**	$[C_{24}H_{30}O_2S_2 + Na]^+$	1	437.158	−0.01
II	0.02	445.15	**7a**	$[C_{22}H_{30}O_4S_2 + Na]^+$	2	445.148	0.00
X	0.01	447.16	**7b**	$[C_{22}H_{32}O_4S_2 + Na]^+$	2	447.163	0.00
XI	0.01	453.15	**1b**	$[C_{24}H_{30}O_3S_2 + Na]^+$	1	453.153	0.00
XII	0.07	463.25	**12b**	$[C_{23}H_{36}O_4S_2 + Na]^+$	2	463.195	0.05
III	0.12	469.18	**15**	$[C_{23}H_{42}O_8 + Na]^+$	3	469.28	−0.10
XIII	0.01	505.15					
XIV	0.01	543.28	**1**	$[C_{31}H_{42}O_4S_2 + H]^+$	2	543.260	0.02
XV	0.02	549.27	**1a**	$[C_{31}H_{42}O_5S + Na]^+$	2	549.265	0.01

[a] See Schemes 3−6 and 8 for the corresponding product ion structures.

and theoretical *m*/*z* values (m/z_{exp} and m/z_{theo}, respectively), the polymer ion assignments, the corresponding molecular formulas and the *m*/*z* errors. All poly(BA) product ion assignments are analogous to the poly(MA) product ion assignments presented in the above Schemes 3−7.

Once again, the set of dithioester initiated polymer product ions **7a** and **7b** are observed (see Figure 3 and Table 3, peaks II and IV, respectively) supporting further the importance of dithioester initiation during CPDA-mediated acrylate polymerizations initiated via γ-irradiation. Interestingly, polymer product ion **7b** is observed only as a doubly charge sodium adduct. Additionally, the main polymer product ion **1** (the cumyl initiated polymer chain end-capped via phenyl dithioacetate) and its analogue **1d**, which may result from cleavage of the Z-group due to interactions with γ-radiation, (peaks I and IX, respectively) are observed. However, ions **1d** and **5c** have identical molecular formulas, and thus, molecular weights and since polymer product ion **5a** is clearly identified and abundant (Table 3, peak VI), no distinction is possible.

Another example of polymer product ions due to water radiolysis and subsequent HO$^\bullet$ initiation is observed (peak VIII

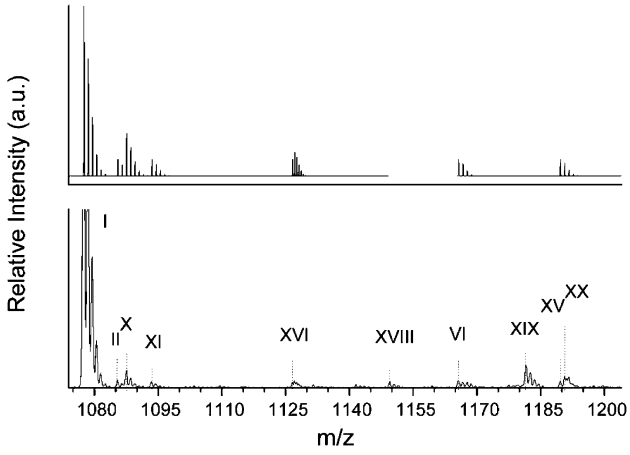

Figure 5. Spectrum of poly(butyl acrylate) obtained from the electrospray ionization mass spectrometry of a reversible addition fragmentation chain transfer mediated BA in 50 vol % toluene polymerization initiated via ^{60}Co γ-irradiation at room temperature. The lower graph presents an expanded view of the mass range 1073 − 1203 Da. The upper part presents the theoretical isotopic pattern for the proposed polymer product ions. Polymer products were analyzed using a quadrupole ion trap mass spectrometer.

species **13f**) (see Scheme 7). To test the importance of water radiolysis during ^{60}Co γ-irradiation, 10 μL of water was added to the BA monomer prior to γ-irradiation. Unfortunately this amount of water, albeit small, caused the formation of cross-linked polymer possibly due to hydrolysis of the RAFT agent. Thus, if water initiation is occurring in this system, it most likely comes from condensation of water under ambient conditions.

The BA polymerization also produces polymer product ions that may originate from interaction of the γ-irradiation with the BA monomer. Within instrument error, polymer product ions **17a** and **15** are observed in the polymer product spectrum (Figure 3). Unfortunately, *m*/*z* value overlap with the polymer product ion **1** renders identification of the methoxy initiated product ions **15a** or **15b** difficult. Additionally, evidence for methyl acrylate monomer interactions with γ-irradiation is lacking. For a more complete list of potential polymer product ions that could arise from initiating species generated via BA (and where analogous, MA) monomer and γ-interactions, please see Scheme S8 in the Supporting Information section.

Butyl Acrylate:Hybrid Quadrupole−Time-of-Flight Mass Spectrometer. To aid in identifying the unknown peaks and the peaks with multiple assignments a Q−ToF instrument was used to examine the same polymer product presented in Figure 3 obtained for the CPDA-mediated BA polymerization initiated via γ-irradiation. Figure 4 presents the spectrum for an expanded view of the mass range 435−565 Da (lower part, where the *y*-axis is scaled to allow for better viewing of the minor peaks) along with the theoretical isotopic pattern for the polymer product ions (upper part). Additionally, Table 4 displays the polymer peaks along with the normalized peak intensities (normalized to the peak intensity of species **1**, Scheme 1), the experimental and theoretical *m*/*z* values (m/z_{exp} and m/z_{theo}, respectively), the polymer ion assignments, the corresponding molecular formulas and the *m*/*z* errors.

Once again, species **7a** and **7b** are observed (Table 4 peaks II and X, respectively) with negligible *m*/*z* assignment error supporting further the importance of dithioester initiation during CPDA-mediated ^{60}Co γ-irradiation. Additionally, the main RAFT product ion **1** is found cationized by both sodium and hydrogen (peaks I and XIV, respectively) and the oxidized main RAFT product ions **1a** and **1b** are identified as peaks XV and

Table 5. Polymer Peaks along with Normalized Peak Intensities (norm. int., Normalized to the Peak Intensity of Species 1, Scheme 1), the Experimental and Theoretical *m*/*z* Values (m/z_{exp} and m/z_{theo}, Respectively), the Ion Assignments (ion assign.), the Molecular Formulas, the Number of Monomer Units Associated with the Ion Assignments (*n*) and the *m*/*z* Errors for Poly(butyl Acrylate) Obtained from the Reversible Addition Fragmentation Chain Transfer Mediated BA in 50 vol % Toluene Polymerization Initiated via ^{60}Co γ-Irradiation at Room Temperature and Analyzed Using a Quadrupole Ion Trap Mass Spectrometer[a]

peak	norm. int.	m/z_{exp}	ion assign.	molecular formula	*n*	m/z_{theo}	$m/z_{exp} - m/z_{theo}$
I	1.00	1077.52	**1**	$[C_{59}H_{90}O_{12}S_2 + Na]^+$	6	1077.577	−0.06
II	0.01	1085.45	**7a**	$[C_{57}H_{90}O_{14}S_2 + Na]^+$	7	1085.566	−0.12
X	0.02	1087.59	**7b**	$[C_{57}H_{92}O_{14}S_2 + Na]^+$	7	1087.582	0.00
XI	0.01	1093.45	**1b**	$[C_{59}H_{90}O_{13}S_2 + Na]^+$	6	1093.572	−0.12
XVI	0.01	1126.60	**1**	$[C_{122}H_{198}O_{30}S_2 + Na_2]^{2+}$	15	1126.660	−0.06
XVIII	0.01	1149.52					
VI	0.003	1165.69	**5a**	$[C_{65}H_{106}O_{16} + Na]^+$	8	1165.737	-0.05
XIX	0.03	1181.57					
XV	0.01	1189.67	**1a**	$[C_{66}H_{102}O_{15}S + Na]^+$	7	1189.684	-0.01
XX	0.01	1190.65					

[a] See Schemes 3−5 for the corresponding product ion structures.

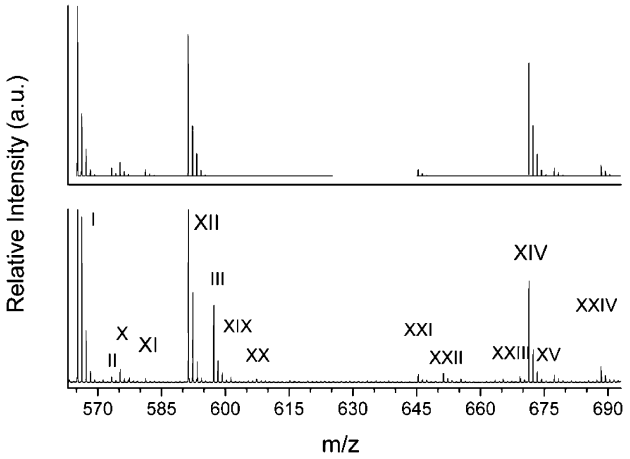

Figure 6. Spectrum of poly(butyl acrylate) obtained from the electrospray ionization mass spectrometry of a reversible addition fragmentation chain transfer mediated BA in 50 vol % toluene polymerization initiated via ^{60}Co γ-irradiation at room temperature. The lower part presents an expanded view of the mass range 563−693 Da. The upper part presents the theoretical isotopic pattern for the polymer product ions. Polymer products were analyzed using a hybrid quadrupole-time-of-flight mass spectrometer.

XI, respectively. Furthermore, the improved peak resolution of the Q−ToF MS allows for clear identification that peak III is not polymer product ion **15** as the error is in excess of 0.05 Da.

Interestingly, peak XII is due to species **12b** (see Scheme 6), indicating that thiol end groups are formed. This process is also suspected to occur during MA polymerization, i.e., as it is possible to assign species **12g** and **12b** to peaks II and XI presented in Table 1 within experimental error; however, more conclusive evidence is necessary to establish the importance of this mechanism. Additionally, no assignment was made for the very weak polymer product peak XIII.

Butyl Acrylate in 50 vol % Toluene:Quadrupole Ion Trap Mass Spectrometer. Solvent polymerization initiated via ^{60}Co γ-irradiation are often performed; thus, the impact of toluene on the RAFT-mediated BA polymerization was investigated. Low molecular weight polymer was obtained from the CPDA-mediated BA polymerization in a 50 vol % toluene mixture initiated via ^{60}Co γ-irradiation. Figure 5 presents the polymer product spectrum obtained using a quadrupole ion trap mass spectrometer along with the theoretical isotopic pattern for the polymer product ions (upper part). As before, the peaks that

Table 6. Polymer Peaks along with Normalized Peak Intensities (norm. int., Normalized to the Peak Intensity of Species 1, Scheme 1), the Experimental and Theoretical *m*/*z* Values (m/z_{exp} and m/z_{theo}, Respectively), the Ion Assignments (ion assign.), the Molecular Formulas, the Number of Monomer Units Associated with the Ion Assignments (*n*), and the *m*/*z* Errors for Poly(BA) Obtained from the Reversible Addition Fragmentation Chain Transfer Mediated BA in 50 vol % Toluene Polymerization Initiated via ^{60}Co γ-Irradiation at Room Temperature and Analyzed Using a Hybrid Quadrupole−Time-of-Flight Instrument[a]

peak	norm. int.	m/z_{exp}	ion assign.	molecular formula	*n*	m/z_{theo}	$m/z_{exp} - m/z_{theo}$
I	1.00	565.24	**1**	$[C_{31}H_{42}O_4S_2 + Na]^+$	2	565.24	0.00
II	0.01	573.25	**7a**	$[C_{29}H_{42}O_6S_2 + Na]^+$	3	573.23	0.01
X	0.01	575.26	**7b**	$[C_{29}H_{44}O_6S_2 + Na]^+$	3	575.25	0.01
XI	0.01	581.26	**1b**	$[C_{31}H_{42}O_5S_2 + Na]^+$	2	581.24	0.02
XII	0.48	591.33	**12b**	$[C_{30}H_{48}O_6S_2 + Na]^+$	3	591.28	0.06
III	0.14	597.27					
XIX	0.01	601.34					
XX	0.01	607.35					
XXI	0.01	645.36	**22c**	$[C_{34}H_{54}O_8S + Na]^+$	4	645.34	0.01
XXII	0.01	651.29					
XXIII	0.01	669.34					
XIV	0.12	671.35	**1**	$[C_{38}H_{54}O_6S_2 + H]^+$	3	671.34	0.00
XV	0.01	677.35	**1a**	$[C_{38}H_{54}O_7S + Na]^+$	3	677.35	0.00
XXIV	0.02	688.37	**1**	$[C_{38}H_{54}O_6S_2 + NH_4]^+$	3	688.37	0.00

[a] See Schemes 3−6 and 9 for the corresponding product ion structures.

Scheme 8. Sodium Adducts from Electrospray of Cumyl Phenyl Dithioacetate Mediated Butyl Acrylate Polymer Initiated via ^{60}Co γ-Irradiation: Initiating Species That Arise Due to Monomer and γ-Radiation Interactions[a]

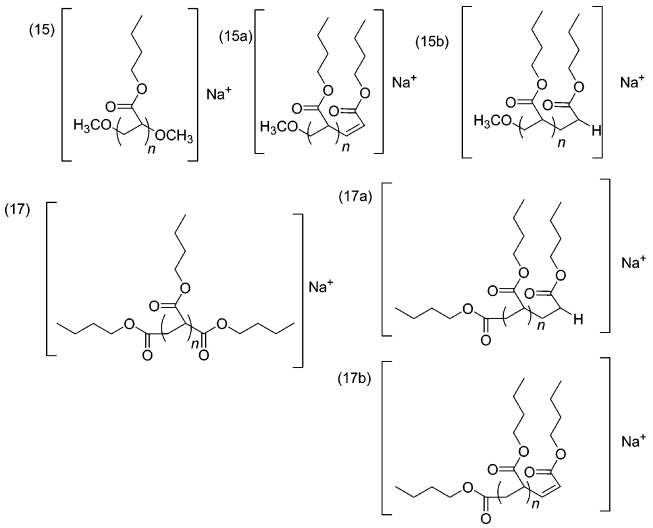

[a] See Scheme S8 in the Supporting Information for a more complete list.

repeat throughout the spectrum are labeled with a Roman numeral (lower part, where the *y*-axis is scaled to allow for better viewing of the minor peaks). Additionally, Table 5 displays the polymer peaks along with the normalized peak intensities (normalized to the peak intensity of species **1**, Scheme 1), the experimental and theoretical *m*/*z* values (m/z_{exp} and m/z_{theo}, respectively), the polymer ion assignments, the corresponding molecular formulas, the degree of polymerization of the polymer ion presented and the *m*/*z* errors.

The addition of 50 vol % toluene does not impact the importance of dithioester initiation during CPDA-mediated BA polymerization initiated via ^{60}Co γ-irradiation; i.e., polymer product ions **7a** and **7b** are observed again (peaks II and X, respectively). While, at first glance, the error for assigning peak II as **7a** may appear in excess of the instrument error (∼0.1 Da), an *m*/*z* error of −0.06 is obtained for ion **1**, which is a known peak. When the error for ion **1** is accounted for, the molecular formula for peak II is assigned with confidence.

Scheme 9. Potential Sodium Adducts from Electrospray of Cumyl Phenyl Dithioacetate Mediated 50/50 vol % Butyl Acrylate/Toluene Polymerization Initiated via ^{60}Co γ-Irradiation.

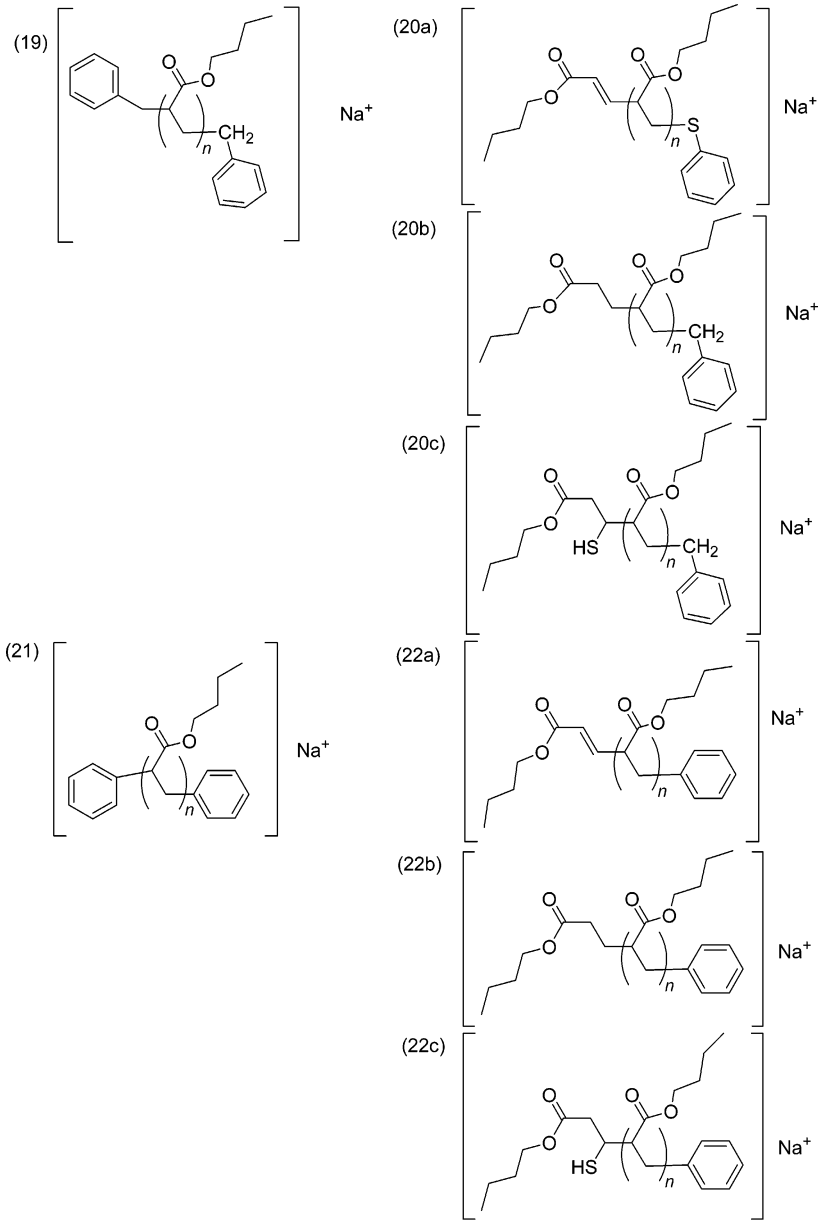

Notably, peak VI, species **5a**, which was a significant portion of the polymer product during the bulk BA polymerization (see Figure 3), again is observed. Additionally, the main RAFT polymer product ion (**1**) is found both singly and doubly charged, and the oxidized main RAFT product ions **1a** and **1b** are identified as peaks XV and XI, respectively. Last, new unknown peaks XVIII, XIX and XX are observed; however, peak XIX and peak VII from Table 3 differ in molar mass by exactly 2 Da, which is characteristic of a set of disproportionation peaks.

BA in 50 vol % Toluene:Hybrid Quadrupole−Time-of-Flight Mass Spectrometer. To complete the analysis of the ^{60}Co γ-initiated BA polymerization in 50 vol % toluene with 0.02 M CPDA, the sample was analyzed using a Q−ToF mass spectrometer. Figure 6 presents the polymer product spectrum along with the theoretical isotopic pattern for the polymer product ions (upper part). The peaks that repeat throughout the mass spectrum are labeled with a roman numeral (lower part, where the *y*-axis is scaled to allow for better viewing of the minor peaks). Additionally, Table 6 displays the polymer peaks along with the normalized peak intensities (normalized to the peak intensity of species **1**, Scheme 1), the experimental and theoretical *m*/*z* values (m/z_{exp} and m/z_{theo}, respectively), the polymer ion assignments, the corresponding molecular formulas, and the *m*/*z* errors.

The importance of dithioester initiation is emphasized as the phenyl dithioacetate initiated polymer product ions **7a** and **7b** are observed (peaks II and X, respectively; see Figure 6). Interestingly, a new peak XXI is observed and is assigned to structure **22c** presented in Scheme 9; however, this assignment is made hesitantly as the polymer product ions **22**, **22a**, and/or **22b** are not observed. Additionally, peak XII is ion **12b** (Scheme 6), which provides additional evidence that thiol end groups form and are important. Again, peaks I, XIV, and XXIV are the main polymer product ion **1** ionized by Na^+, H^+ and NH_4^+, respectively, and the oxidized main RAFT product ions **1a** and **1b** (peaks XV and XI, respectively) are observed. Last, no new information for peaks VI, XVII, and XVIII is gained, peaks

Scheme 10. Summary of Initiation Processes That Occur during Cumyl Phenyl Dithioacetate Mediated Acrylate Polymerizations Initiated via ^{60}Co γ-Irradiation

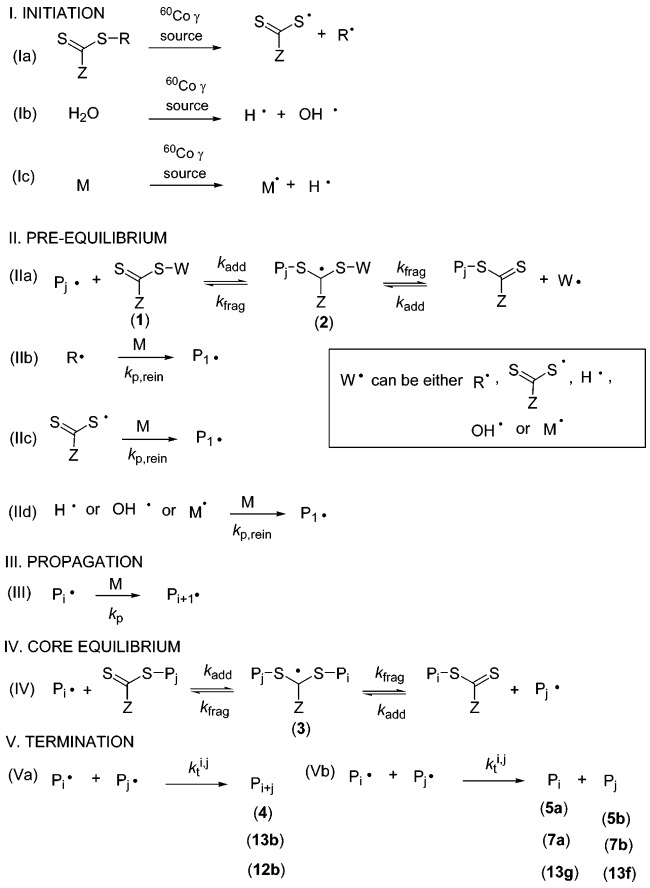

III, XIX, and XX remain unknown and two new peaks, XXII and XXIII, are observed.

Mechanistic Summary. Information about the γ-initiation mechanism during CPDA-mediated methyl and butyl acrylate polymerizations initiated via ^{60}Co γ-irradiation is gained using electrospray ionization mass spectrometry and is summarized in Scheme 10, which presents the modified RAFT mechanism (modified from the RAFT mechanism presented in Scheme 1). Specifically, the initiation and pre-equilibrium mechanisms are modified to account for water radiolysis (reaction Ib), which yields the initiating species H$^\bullet$ and HO$^\bullet$, and for monomer interactions with γ-irradiation to yield a monomer based initiating species, M$^\bullet$ (reaction Ic). Additionally, the pre-equilibrium steps (reactions IIc and IId) account for dithioester radical, H$^\bullet$, HO$^\bullet$, or M$^\bullet$ initiation of polymer chains. These radicals can also enter into the pre-equilibrium reaction II. However, it should be noted that this is merely a possibility, as we have not sought to identify the presence of variable RAFT agents during the early part of the reaction. Finally, the termination mechanism reaction V describes the potential combination (Va) and disproportionation (Vb) products. As expected, no polymer product ions indicative of the cross-termination reactions Vc and Vd were observed.[41]

Scheme 11 presents the polymer product ions that were found in both the MA and BA polymer product spectra, where Y is either CH_3 or C_4H_9 for either MA or BA, respectively. Additionally, the polymer product ions that are observed for only the BA polymerization, i.e., species **17a** initiated via a molecule that arises from BA monomer and γ-radiation interactions, and species **12b**, which is formed due to thiol end group and disulfide bond formations, are presented.

For each polymerization, the main peaks generated from ESI of the γ-initiated samples are due to species **1** (Scheme 10), which forms via the generally assumed RAFT process that utilizes reactions Ia, IIa, IIb, III, and IV. Species **1** is observed also as a doubly charged sodium adduct when the quadrupole ion trap mass spectrometer is used (Table 1, peaks V and XII, and Table 5, peak XVI) and as a hydrogen adduct (Tables 4 and 6, peak XIV) or ammonium adduct (Table 6, peak XXIV) when the Q−ToF instrument is used. Oxidation of species **1**, i.e., species **1a** and **1b**, is observed also for methyl acrylate (Tables 1 and 2, peaks XI and III, respectively) and butyl acrylate (Tables 4 and 6, peaks XV and XI, respectively) polymerizations and is observed using either the Q−ToF or the quadrupole ion trap instruments.

Additionally, the polymer product ion **1d** is observed (Tables 1 and 2 peak VII and Table 3 peak IX). This species may arise due to the C−S bond on the dithioester group of species **1** cleaving to generate a thiol end group. Further evidence of C−S bond cleavage is gained upon observation of species **12b** (Tables 4 and 6, peak XII), which is proposed to generate when a disulfide bond forms between species **1d** and species **7b** (post cleavage of its C−S bond). However, species **12b** could also form via a disulfide bond formation between species **1d** and a thiol initiated species (**12g**).

Importantly, product ions indicative of dithioester initiation (i.e., species **7a** and **7b**) are observed in all spectra (Tables 1 and 2, peaks VIII and IX, respectively, and Tables 3−6, peaks II and X, respectively). While dithioester initiated polymer chains were observed in all of the spectra, the polymer product is clearly dominated by cumyl initiated chains end-capped by a dithioester group; thus, the release of R$^\bullet$ groups via reaction IIa in the RAFT mechanism (Scheme 1) must be faster than the reaction I in the reversible termination mechanism (Scheme 2). Also, product ion **7b** is observed as a hydrogen adduct when the poly(MA) sample is analyzed via the Q−ToF (Table 2, peak VI). Additionally, species **7b** forms as a doubly charged sodium adduct with poly(BA) when the quadrupole ion trap mass spectrometer is used (Table 3, peak IV).

Furthermore, evidence for cumyl radical initiation (species **5a**) is observed for the MA (Tables 1 and 2, peak II) and BA polymerization in 50 vol % toluene (Table 5, peak VI). However, product ion **5b** is observed for only the MA polymer analyzed using the Q−ToF (Table 2, peak XIV). Additionally, within instrument error, product ion XIV is also species **13b**, which indicates that water radiolysis to form an initiating species is possible (see Scheme 10, reaction 1b). This mechanism is supported further by the presence of species **13f** in the poly(BA) spectra obtained using the quadrupole ion trap mass spectrometer (Table 3, peak VIII). Finally, the polymer product ion **17a** is observed for the poly(BA) polymerizations (Table 3 peak V), indicating the importance of initiation mechanism (Ic), i.e., the formation of initiating species via interactions between monomer and γ-irradiation.

Conclusions

Cumyl phenyl dithioacetate (CPDA) mediated methyl acrylate and butyl acrylate polymerizations initiated via ^{60}Co γ-irradiation are investigated using electrospray ionization mass spectrometry (ESI−MS). Both a quadrupole-time-of-flight instrument and a quadrupole ion trap mass spectrometer were utilized to map the polymer end-groupings. While the Q−ToF clearly provides better isotopic pattern resolution when compared to the quadrupole ion trap instrument, both mass spectrometers

Scheme 11. Summary of Polymer Product Ions from Electrospray Ionization of Cumyl Phenyl Dithioacetate Mediated Acrylate Polymerizations Initiated via ^{60}Co γ-Irradiation

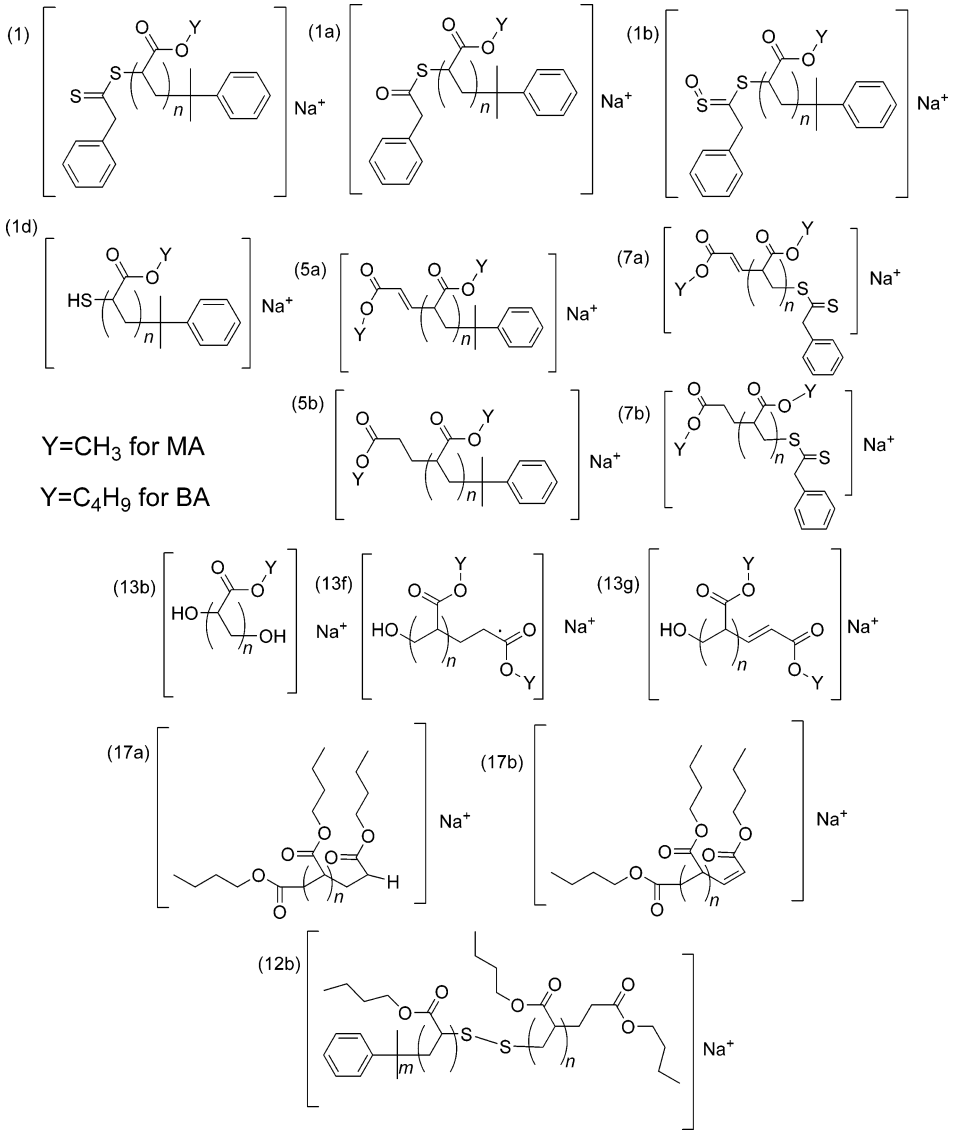

were used to investigate the polymer products because analysis and identification of the minor peaks provides the important-mechanistic information and different polymer product ions are observed using the different mass spectrometers. Three potential initiation processes are identified. Importantly, a set of polymer product ions indicates that a small, yet significant, fraction of the γ-generated phenyl dithioacetate radical (Z-group from CPDA) contributes to the initiation process. Furthermore, the phenyl dithioacetate group undergoes cleavage to yield a thiol radical that either abstracts a hydrogen or reacts to form a disulfide linkage. Polymer product ions indicative of a small amount of water radiolysis are also observed. Additionally, evidence that the butyl acrylate monomer interacts with γ-radiation to yield an initiating species is presented. In conclusion, detailed mechanistic insight into the RAFT-mediated acrylate FRP initiation processes during γ-irradiation is gained through a careful and thorough ESI−MS study that provides invaluable information for the synthetically working chemist with respect to the end groups generated in applications ranging from γ-induced grafting to the formation of polymer protein conjugates.

Acknowledgment. C.B.-K. thanks the Australian Research Council (ARC) for their financial support in the form of a Discovery Grant as well as an Australian Professorial Fellowship. Additionally, we recognize Dr. Leonie Barner and Mr. Istvan Jacenyik for their outstanding management of CAMD. T.P.D. acknowledges receipt of a Federation Fellowship. We also thank A/Prof Mike Guilhaus and Dr. Russ Pickford at the UNSW Bioanalytical Mass Spectrometry Facility (BMSF) for their many helpful discussions and use of the BMSF Ultima hybrid quadrupole-time-of-flight instrument.

Supporting Information Available: Schemes S1−S8, showing possible sodium adducts from electrospray of the polymers. This material is available free of charge via the Internet at http://pubs.acs.org.

References and Notes

(1) Hua, D.; Cheng, K.; Bai, W.; Bai, R.; Lu, W.; Pan, C. *Macromolecules* **2005**, *38*, 3051−3053.
(2) Rybak, A. S.; Grinyuk, E. V.; Kilimets, T. G.; Polikarpov, A. P.; Brazhnikov, M. M.; Shadyro, O. I.; Krul, L. P. *Radiat. Chem.* **2003**, *37*, 265−267.
(3) Zou, M.; Zhang, Z.; Shen, X.; Nie, J.; Ge, X. *Radiat. Phys. Chem.* **2005**, *74*, 323−330.
(4) Nasef, N. M. *J. Appl. Polym. Sci.* **2000**, *77*, 1003−1012.

(5) Pande, C. S.; Gupta, N. *J. Appl. Polym. Sci.* **1999**, *71*, 2163−2168.
(6) El Nesr, E. M.; Dessouki, A. M.; Abdel-Bary, E. M. *Polym. Int.* **1998**, *46*, 150−156.
(7) Sabharwal, S.; Das, T. N.; Chaudhari, C. V.; Y. K. B.; Majali, A. B. *Radiat. Phys. Chem.* **1998**, *51*, 309−315.
(8) Kiryukhin, D. P.; Barkalov, I. M. *Polym. Adv. Tech.* **1996**, *7*, 287−294.
(9) Barner-Kowollik, C.; Davis, T. P.; Heuts, J. P. A.; Stenzel, M. H.; Vana, P.; Whittaker, M. *J. Polym. Sci., Part A: Polym. Chem.* **2003**, *41*, 365−375.
(10) Mayadunne, R. T. A.; Rizzardo, E.; Chiefari, J.; Kristina, J.; Moad, G.; Postma, A.; Thang, S. H. *Macromolecules* **2000**, *33*, 243−245.
(11) Chong, Y. K.; Le, T. P. T.; Moad, G.; Rizzardo, E.; Thang, S. H. *Macromolecules* **1999**, *32*, 2071−2074.
(12) Chiefari, J.; Chong, Y. K.; Ercole, F.; Krstina, J.; Jeffery, J.; Le, T. P. T.; Mayadunne, R. T. A.; Meijs, G. F.; Moad, C. L.; Moad, G.; Rizzardo, E.; Thang, S. H. *Macromolecules* **1998**, *31*, 5559−5562.
(13) Barner, L.; Perera, S.; Sandanayake, S.; Davis, T. P. *J. Polym. Sci., Part A: Polym. Chem.* **2006**, *44*, 857−864.
(14) Barner, L.; Quinn, J. F.; Barner-Kowollik, C.; Vana, P.; Davis, T. P. *Eur. Polym. J.* **2003**, *39*, 449−459.
(15) Barner, L.; Zwaneveld, N.; Perera, S.; Pham, Y.; Davis, T. P. *J. Polym. Sci., Part A: Polym. Chem.* **2002**, *40*, 4180−4192.
(16) Quinn, J. F.; Barner, L.; Rizzardo, E.; Davis, T. P. *J. Polym. Sci., Part A: Polym. Chem.* **2002**, *40*, 19−25.
(17) He, T.; Zou, Y.-F.; Pan, C.-Y. *J. Polym. Sci., Part A: Polym. Chem.* **2002**, *40*, 3367−3378.
(18) He, T.; Zheng, G.-H.; Pan, C.-Y. *Macromolecules* **2003**, *36*, 5960−5966.
(19) Liu, J.; Bulmus, V.; Herlambang, D. L.; Barner-Kowollik, C.; Stenzel, M. H.; Davis, T. P. *Angew. Chem.* **2007**, *46*, 3099−3103.
(20) Quinn, J. F.; Barner, L.; Davis, T. P.; Thang, S. H.; Rizzardo, E. *Macromol. Rapid Commun.* **2002**, *23*, 717−721.
(21) Feldermann, A.; Ah Toy, A.; Davis, T. P.; Stenzel, M. H.; Barner-Kowollik, C. *Polymer* **2005**, *46*, 8448−8457.
(22) Products **3a** and **3b** are—if they occur—only expected to form when highly stabilized RAFT adduct radicals are formed, i. e., when Z = phenyl. In the present study, Z = benzyl. It is not possible to observe polymerization with, e.g., cumyl dithiobenzoate at ambient temperatures due to the large intermediate radical stability causing a strong inhibition phenomenon.
(23) Barner-Kowollik, C.; Buback, M.; Charleux, B.; Coote, M. L.; Drache, M.; Fukuda, T.; Goto, A.; Klumperman, B.; Lowe, A. B.; McLeary, J.; Moad, G.; Monteiro, M. J.; Sanderson, R. D.; Tonge, M. P.; Vana, P. *J. Polym. Sci., Part A: Polym. Chem.* **2006**, *44*, 5809−5831.
(24) Barner-Kowollik, C.; Vana, P.; Quinn, J. F.; Davis, T. P. *J. Polym. Sci., Part A: Polym. Chem.* **2002**, *40*, 1058−1063.
(25) Quinn, J. F.; Rizzardo, E.; Davis, T. P. *Chem. Commun.* **2001**, 1044−1055.
(26) Bai, R.-K.; You, Y.-Z.; Pan, C.-Y. *Macromol. Rapid Commun.* **2001**, *22*, 315−319.
(27) Peacock, P. M.; McEwen, C. N. *Anal. Chem.* **2006**, *78*, 3957−3964.
(28) Xu, J.; He, J.; Fan, D.; Wang, X.; Yang, Y. *Macromolecules* **2006**, *39*, 8616−8624.
(29) Osaka, I.; Watanabe, M.; Takama, M.; Murakami, M.; Arakawa, R. *J. Mass Spec.* **2006**, *41*, 1369−1377.
(30) Scrivens, J. H.; Jackson, A. T. *Int. J. Mass Spectrom.* **2000**, *200*, 261−276.
(31) Vana, P.; Albertin, L.; Barner, L.; Davis, T. P.; Barner-Kowollik, C. *J. Polym. Sci., Part, A.: Polym. Chem.* **2002**, *40*, 4032−4037.
(32) Deery, M. J.; Jennings, K. R.; Jasieczek, C. B.; Haddleton, D. M.; Jackson, A. T.; Yates, H. T.; Scrivens, J. H. *Rapid Commun. Mass Spec.* **1997**, *11*, 57−62.
(33) Rizzarelli, P.; Puglisi, C.; Montaudo, G. *Rapid Commun. Mass Spec.* **2006**, *20*, 1683−1694.
(34) Baker, E. S.; Gidden, J.; Simonsick, W. J.; Grady, M. C.; Bowers, M. T. *Int. J. Mass Spectrom.* **2004**, *238*, 279−286.
(35) Trimpin, S.; Keune, S.; Rader, H. J.; Mullen, K. *J. Am. Soc. Mass Spectrom.* **2006**, *17*, 661−671.
(36) Barner-Kowollik, C.; Davis, T. P.; Stenzel, M. H. *Polymer* **2004**, *45*, 7791−7805.
(37) McEwen, C. N. *J. Am. Soc. Mass Spectrom.* **1995**, *6*, 906−911.
(38) Nguyen, D. C.; Vana, P. *Aust. J. Chem.* **2006**, *59*, 549−559.
(39) Buback, M.; Frauendorf, H.; Vana, P. *J. Polym. Sci., Part, A.: Polym. Chem.* **2004**, *42*, 4266.
(40) Szablan, Z.; Lovestead, T. M.; Stenzel, M. H.; Davis, T. P.; Barner-Kowollik, C. *Macromolecules* **2007**, *40*, 26−39.
(41) Ah Toy, A.; Vana, P.; Davis, T. P.; Barner-Kowollik, C. *Macromolecules* **2004**, *37*, 744−751.
(42) Quan, C.; Soroush, M.; Grady, M. C.; Hansen, J. E.; Simonsick, W. J., Jr. *Macromolecules* **2005**, *38*, 7619−7628.
(43) Jiang, X.; Schoenmakers, P. J.; van Dongen, J. L. J.; Lou, X.; Lima, V.; Brokken-Zijp, J. *Anal. Chem.* **2003**, *75*, 5517−5524.
(44) Jiang, X.; Schoenmakers, P. J.; Lou, X.; Lima, V.; van Dongen, J. L. J.; Brokken-Zijp, J. *J. Chrom. A* **2004**, *1055*, 123−133.
(45) Feldermann, A.; Stenzel, M. H.; Davis, T. P.; Vana, P.; Barner-Kowollik, C. *Macromolecules* **2004**, *37*, 2404−2410.
(46) Hua, D.; Xiao, J.; Bai, R.; Lu, W.; Pan, C. *Macromol. Chem. Phys.* **2004**, *205*, 1793−1799.
(47) You, Y.-Z.; Bai, R.-K.; Pan, C.-Y. *Macromol. Chem. Phys.* **2001**, *202*, 1980−1985.
(48) Bai, R.-K.; You, Y.-Z.; Zhong, P.; Pan, C.-Y. *Macromol. Chem. Phys.* **2001**, *202*, 1970−1973.
(49) Hua, D.; Ge, X.; Bai, R.; Lu, W.; Pan, C. *Polymer* **2005**, *46*, 12696−12702.
(50) Hua, D.; Bai, R.; Lu, W.; Pan, C. *J. Polym. Sci., Part A: Polym. Chem.* **2004**, *42*, 5670−5677.
(51) Barner-Kowollik, C.; Quinn, J. F.; Nguyen, T. L. U.; Heuts, J. P. A.; Davis, T. P. *Macromolecules* **2001**, *34*, 7849−7857.
(52) Quinn, J. F.; Barner, L.; Barner-Kowollik, C.; Rizzardo, E.; Davis, T. P. *Macromolecules* **2002**, *35*, 7620−7627.
(53) Hutson, L.; Kristina, J.; Moad, C. L.; Moad, G.; Morrow, G. R.; Postma, A.; Rizzardo, E.; Thang, S. H. *Macromolecules* **2004**, *37*, 4441−4452.

MA0701484